

Efficient Calculation of the Band Structure of Artificial Materials With Cylindrical Metallic Inclusions

Mário G. Silveirinha, *Student Member, IEEE*, and Carlos A. Fernandes, *Member, IEEE*

Abstract—In this paper, we present a new hybrid method that makes the calculation of the band structure of artificial materials with cylindrical metallic inclusions very efficient. We derive an auxiliary problem whose band structure is that of the metallic crystal along with several dispersionless bands. The eigenfunctions of the auxiliary problem have continuous derivatives up to order 2. Thus, the spectrum of the auxiliary problem can be efficiently computed using the plane-wave method. The band structure of the metallic crystal is then obtained by extracting from the computed results the dispersionless bands.

Index Terms—Artificial materials, band structure, metallic crystals.

I. INTRODUCTION

IN RECENT years, a great interest has arisen in the study of photonic crystals, after the pioneering work of Yablonovitch *et al.* [1]. As is well known, these structures can have a full photonic bandgap (PBG), where the propagation of electromagnetic waves is forbidden in every direction of space and for every polarization state.

The PBG regime emerges when the lattice constant is comparable to the wavelength of radiation. On the other hand, if the wavelength of radiation is much larger than the lattice constant, the photonic crystal can be characterized by an effective permittivity and permeability [2], [3]. This corresponds to the effective medium regime, and is of particular interest for artificial dielectric applications. This concept was thoroughly investigated in the 1960s, and regains interest due to current advances in micro-fabrication techniques. At the long wavelength regime, the artificial material can be characterized using quasi-static methods [3]. Despite that fact, and in order to predict the dependence of the effective permittivity permeability with frequency, the calculation of the fundamental bands of the periodic structure is of great relevance.

The propagation of electromagnetic waves in periodic structures is described by means of a band theory. The computation of the band structure is, in general, very intensive. Several methods have been proposed for the effect, i.e., the order- N

Manuscript received April 12, 2002; revised November 9, 2002. This work was supported by the Fundação para Ciência e a Tecnologia under Project POSI 34860/99.

M. G. Silveirinha is with the Electrical Engineering Department, University of Coimbra, 3030 Coimbra, Portugal (e-mail: mario.silveirinha@co.it.pt).

C. A. Fernandes is with the Instituto Superior Técnico, Technical University of Lisbon, 1049-001 Lisbon, Portugal (e-mail: carlos.fernandes@lx.it.pt).

Digital Object Identifier 10.1109/TMTT.2003.810150

method [4], the transfer matrix method (TMM) [5], finite-difference methods [6], plane-wave method [7], [8], etc.

The order- N method is based on the finite-difference time-domain (FDTD) method. The time-dependent Maxwell equations are solved for given initial conditions and boundary conditions. The spectral intensity, whose peaks correspond to the resonant frequencies, is then computed using a Fourier transform. An important feature of this method is that the computational effort scales linearly with the size of the system.

The TMM is a multiscattering method, and allows for the computation of the complex band structure and reflection-transmission coefficients in truncated crystals.

The plane-wave method involves the expansion of the electromagnetic fields in a Fourier-like series. The Maxwell equations are reduced into a matrix eigensystem. The eigenvectors represent the electromagnetic Floquet modes and the eigenvalues represent the respective resonant frequencies. Nonetheless, this method is restricted to dielectric crystals since it assumes the medium permittivity to be finite and nondispersive.

Indeed, the plane-wave method suffers from convergence problems that are particularly acute for high dielectric contrasts, near close-packing ratios, and high frequencies [8], [9]. A crystal with perfect electric conductors (PECs) can, in principle, be regarded as the limit situation of a dielectric crystal with infinite permittivity inclusions. However, as the dielectric contrast in this configuration is infinite, the plane-wave method fails completely.

The slow convergence of the plane-wave method is related to the discontinuity of the dielectric constant and, consequently, of the electromagnetic fields. These discontinuities cause the plane-wave expansions of the pertinent physical quantities to fluctuate intensely around the dielectric interfaces, in a manifestation of the Gibbs phenomenon. Thus, a very large number of plane waves may be required for the accurate computation of the band structure of a dielectric crystal. This is memory and time consuming since the number of operations for diagonalizing a Hermitian matrix scales as the cube of the dimension.

In metallic crystals, the discontinuous behavior of the electromagnetic fields is even more critical. Indeed, if the inclusions are perfect conductors, the boundary conditions impose not only the normal component of the electric field to be discontinuous, but also the tangential component of the magnetic field. In this paper, we prove that, in spite of the referred irregular behavior, it is possible to compute very efficiently the band structure of metallic crystals with PEC inclusions using a hybrid plane-wave integral-equation-based method. The analysis of this paper is

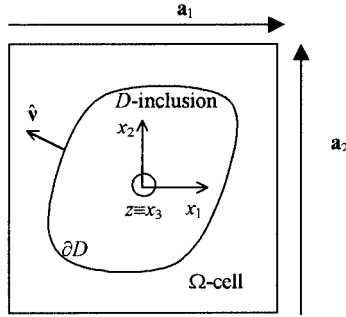


Fig. 1. Unit cell in the square lattice case. The metallic inclusion is D and the lattice primitive vectors are \mathbf{a}_1 and \mathbf{a}_2 .

restricted to cylindrical inclusions with arbitrary cross section. The general three-dimensional and dielectric cases [10] will be presented elsewhere.

The proposed method is described below. To begin, we introduce an auxiliary extended problem. The band structure of this problem contains that of the metallic crystal, along with a set of dispersionless flat bands. The flat bands are associated to the resonant frequencies of the interior Dirichlet problem in a metallic waveguide with the same cross section as a generic inclusion. We prove that the extended problem is equivalent to an integral-differential eigensystem. The eigenfunctions of this eigensystem are smooth and, thus, can be expanded into a fast converging Fourier series. In this way, the band structure of the extended problem can be efficiently computed using the plane-wave method. As the flat bands do not depend on the wave vector, they can be easily extracted from the band structure of the extended problem, thus leaving the band structure of the metallic crystal. The proposed method is partially related to the boundary integral resonant method [11], [12], which is utilized for the calculation of the resonant modes in metallic waveguides.

Previous work on the analysis of metallic crystals includes [13], where the band structure of an array of PEC cylinders is calculated using a generalized Rayleigh identity method, [14] which uses the TMM method, and [15], which studies the dispersive case.

This paper is organized as follows. In Section II, we present the formulation of the method. In Section III, we present numerical results. In Section IV, we present conclusions.

II. FORMULATION

We consider a two-dimensional lattice of metallic cylinders in air. The lattice primitive vectors are \mathbf{a}_1 and \mathbf{a}_2 . We take the unit cell as the parallelogram $\Omega = \{\alpha_1 \mathbf{a}_1 + \alpha_2 \mathbf{a}_2 : |\alpha_i| \leq 1/2\}$. The square lattice case is depicted in Fig. 1. Inside the unit cell is an infinite PEC metallic cylinder with arbitrary cross section D . We denote the inclusion's boundary by ∂D , and the corresponding outward unit normal vector by $\hat{\mathbf{v}}$. The periodic (metallic) crystal is obtained by translations of Ω along the primitive vectors. For convenience, we introduce the reciprocal lattice [16] primitive vectors \mathbf{b}_1 and \mathbf{b}_2 , defined by the relations $\mathbf{a}_m \cdot \mathbf{b}_n = 2\pi\delta_{m,n}$, where $\delta_{m,n}$ is the Kronecker delta symbol.

The objective is to compute the Floquet electromagnetic modes. We can assume without loss of generality that the

wave vector is normal to the cylinders axes. In the general case, the Floquet wave solutions can be constructed from the solutions of the on-plane case, in analogy with the propagation of electromagnetic waves in PEC metallic waveguides [17]. In fact, the metallic crystal can be regarded as a metallic waveguide with infinite inner conductors. From this remark, it is evident that the metallic crystal supports infinite transverse electromagnetic waves and, in addition, E -polarized waves (transverse magnetic to z) and H -polarized waves (transverse electric to z).

In the on-plane case, the geometry of the problem is intrinsically two-dimensional, and the coordinate along the cylinder axes can be discarded. Thus, we denote a generic observation point by $\mathbf{r} = (x_1, x_2)$.

We put $\psi = E_z$ in the E -polarization case, and $\psi = H_z$ in the H -polarization case. In order to be a Floquet wave, ψ must satisfy

$$\nabla^2\psi + \beta^2\psi = 0 \quad (1)$$

$$\psi^+ = 0, \quad \text{on } \partial D \text{ (}E\text{-polarization)} \quad (2a)$$

$$\partial\psi^+/\partial\mathbf{v} = 0, \quad \text{on } \partial D \text{ (}H\text{-polarization)} \quad (2b)$$

$$\psi \exp(j\mathbf{k} \cdot \mathbf{r}) \text{ is periodic} \quad (3)$$

where $\mathbf{k} = (k_1, k_2)$ is the wave vector, $\partial/\partial\mathbf{v}$ is the normal derivative, ∇ is the (transversal) gradient, $\beta = \omega/c$ is the free-space wavenumber, ω is the angular frequency of radiation, and c is the velocity of light in vacuum. In the E -polarization case, ψ satisfies the Dirichlet boundary condition (2a) at the inclusions' surface, while in the H -polarization case, it satisfies the Neumann boundary condition (2b). The superscript “+” in these equations indicates that the corresponding field quantities are to be evaluated at the outer side of ∂D .

For a given \mathbf{k} in the reciprocal space, system (1)–(3) has non-trivial solutions for an infinite numerable set of wavenumbers. We can write $\beta = \beta(\mathbf{k})$, being the previous function multi-valued. Each branch of the function $\beta(\mathbf{k})$ yields a band. The objective is to determine the band structure.

In the general off-plane case, the wave vector has a longitudinal component, and the dispersion characteristic satisfies $\beta^2(k_1, k_2, k_3) = \beta^2(k_1, k_2, 0) + k_3^2$, being the notation evident. Thus, in PEC metallic crystals, the band structure of the on-plane case determines the band structure of the off-plane case.

A. Extended Problem

In (1), ψ is defined only outside the PEC inclusions. Nevertheless, ψ can be mathematically extended to the interior of the inclusions as a continuous solution of (1) in all space. In the E -polarization case, the last assertion is clear: we just need to define $\psi = 0$ inside the inclusions. The H -polarization case is a bit more elaborated and is treated as follows. We can obviously restrict the analysis to the unit cell. Let ψ^+ be ψ calculated at the outer side of ∂D , and ψ^- be ψ calculated at the inner side of the ∂D . We then define ψ inside D as the solution of (1) that satisfies the boundary condition $\psi^+ = \psi^-$ on ∂D (i.e., ψ is the solution of an interior Dirichlet problem).

We introduce an extended problem, whose solutions are the continuous functions that verify (1)–(3) in all space (including

the interior of the inclusions). The objective will become clear in the following section. The Floquet solutions of the extended problem are the Floquet solutions of the metallic crystal, (extended continuously to the interior of D , as explained earlier), along with a set of internal modes that vanish in the exterior of the inclusions.

As the solutions of the extended problem are continuous, the internal modes vanish at the boundary of the metallic inclusions, independently of the wave polarization. Therefore, the internal modes can be identified with the Dirichlet modes of a metallic waveguide with the same cross section as a generic inclusion. The internal modes are independent of the wave vector and wave polarization.

Thus, the band structure of the extended problem is equal to the band structure of the metallic crystal, together with a set of flat bands that correspond to the resonant frequencies of the interior Dirichlet modes. We can obtain the band structure of the metallic crystal by extracting the flat bands from the band structure of the extended problem. Alternatively, we can check if a given resonant frequency belongs to the band structure of the metallic crystal by testing if the corresponding eigenfunction is zero in $\Omega - D$ (i.e., in the unity cell excluding the inclusion).

The eigenfunctions of the extended problem are continuous, i.e., $[\psi] \equiv \psi^+ - \psi^- = 0$. On the other hand, the first-order derivatives are discontinuous on ∂D . This causes a Fourier expansion of ψ to converge slowly. To circumvent this situation, we derive in the following section an integral-differential eigen-system with the same band structure as the extended problem, but with smoother eigenfunctions.

B. Band Structure of the Extended Problem

Let ψ be an arbitrary extended solution of (1)–(3), i.e., continuous in all space. We consider an auxiliary function ϕ that satisfies

$$\nabla^2 \phi = -\beta^2 \psi \quad (4a)$$

$$\phi \exp(j\mathbf{k} \cdot \mathbf{r}) \text{ is periodic.} \quad (4b)$$

We note that as ψ is continuous, ϕ has continuous derivatives up to the second order in the unit cell (including the boundary of the inclusion ∂D). In what follows, we prove that ϕ is solution of an integral-differential eigensystem.

To begin with, we define

$$\theta = \psi - \phi. \quad (5)$$

From (1)–(5), we obtain that, for an arbitrary point \mathbf{r} in $\Omega - \partial D$

$$\nabla^2 \theta = 0, \quad \text{in } \Omega - \partial D \quad (6a)$$

$$\theta \exp(j\mathbf{k} \cdot \mathbf{r}) \text{ is periodic.} \quad (6b)$$

Although (6a) is a homogeneous equation, θ is nontrivial because, on ∂D , its normal derivative is discontinuous, i.e., $[\partial\theta/\partial\mathbf{\nu}] = \partial\theta^+/\partial\mathbf{\nu} - \partial\theta^-/\partial\mathbf{\nu} \neq 0$ (although θ is continuous, i.e., $[\theta] = \theta^+ - \theta^- = 0$). These results follow from the fact of ψ being a continuous function with discontinuous normal derivative on the inclusion boundary, and ϕ having continuous derivatives up to order 2.

In order to obtain an integral representation for θ , we introduce the lattice Green function $\Phi_p(\mathbf{r}|\mathbf{r}')$ solution of

$$\nabla^2 \Phi_p = -e^{-j\mathbf{k} \cdot (\mathbf{r} - \mathbf{r}')} \sum_{\mathbf{I}} \delta(\mathbf{r} - \mathbf{r}' - \mathbf{r}_{\mathbf{I}}) \quad (7a)$$

$$\Phi_p \exp(j\mathbf{k} \cdot (\mathbf{r} - \mathbf{r}')) \text{ is a periodic function.} \quad (7b)$$

In (7), $\mathbf{r} = (x_1, x_2)$ is an observation point, $\mathbf{r}' = (x'_1, x'_2)$ is a source point, $\mathbf{I} = (i_1, i_2)$ is a multiindex of arbitrary integers, and $\mathbf{r}_{\mathbf{I}} = i_1 \mathbf{a}_1 + i_2 \mathbf{a}_2$ is a lattice point. The details on the computation of the Green function are presented in the Appendix.

From (6) and (7), we obtain the following identity:

$$\nabla' \cdot (\nabla' \Phi_p \theta - \Phi_p \nabla' \theta) = -\theta(\mathbf{r}') e^{-j\mathbf{k} \cdot (\mathbf{r} - \mathbf{r}')} \sum_{\mathbf{I}} \delta(\mathbf{r} - \mathbf{r}' - \mathbf{r}_{\mathbf{I}}) \quad (8)$$

where the prime indicates that the gradient operates over the \mathbf{r}' -coordinates. From (6b), we have that $\theta(\mathbf{r} - \mathbf{r}_{\mathbf{I}}) \exp(-j\mathbf{k} \cdot \mathbf{r}_{\mathbf{I}}) = \theta(\mathbf{r})$ for every lattice point $\mathbf{r}_{\mathbf{I}}$. Therefore, the right-hand side of the above equation simplifies to

$$\nabla' \cdot (\nabla' \Phi_p \theta - \Phi_p \nabla' \theta) = -\theta(\mathbf{r}) \sum_{\mathbf{I}} \delta(\mathbf{r} - \mathbf{r}' - \mathbf{r}_{\mathbf{I}}). \quad (9)$$

Next, we integrate (in order to \mathbf{r}') both sides of (9) over the unit cell Ω . The integral of the right-hand side is $-\theta(\mathbf{r})$. The integral of the left-hand side term can be transformed into two surface integrals: one over ∂D and the other over the boundary of Ω . This last integral vanishes since, from (6b) and (7b), the term inside the divergence operator in (9) is a periodic function in \mathbf{r}' . Hence, we obtain that

$$\theta(\mathbf{r}) = \int_{\partial D} \frac{\partial \Phi_p}{\partial \mathbf{\nu}'}(\mathbf{r}|\mathbf{r}') [\theta] - \left[\frac{\partial \theta}{\partial \mathbf{\nu}'} \right] \Phi_p(\mathbf{r}|\mathbf{r}') ds', \quad \mathbf{r} \in \Omega - \partial D. \quad (10)$$

In (10), the terms in brackets are the jump discontinuities of θ and of its normal derivative at the boundary of the inclusion. Since $[\theta] = 0$, we conclude [remembering the definition of θ in (5)] that

$$\psi(\mathbf{r}) = \phi(\mathbf{r}) + \int_{\partial D} f(\mathbf{r}') \Phi_p(\mathbf{r}|\mathbf{r}') ds' \quad (11a)$$

$$f = - \left[\frac{\partial \theta}{\partial \mathbf{\nu}} \right] = - \left[\frac{\partial \psi}{\partial \mathbf{\nu}} \right] = \frac{\partial \psi^-}{\partial \mathbf{\nu}} - \frac{\partial \psi^+}{\partial \mathbf{\nu}}. \quad (11b)$$

In the former equation, f is a density defined over ∂D . The second term of the right-hand side of (11a) is a (pseudoperiodic) single-layer potential.

Using (2) and (11a), we easily obtain an integral equation for f in terms of ϕ . In fact, if $\mathbf{r} \in \partial D$, we have

$$0 = \phi(\mathbf{r}) + \int_{\partial D} f(\mathbf{r}') \Phi_p(\mathbf{r}|\mathbf{r}') ds' \quad (E\text{-pol.}) \quad (12a)$$

$$0 = \frac{\partial \phi}{\partial \mathbf{\nu}}(\mathbf{r}) + \int_{\partial D} f(\mathbf{r}') \frac{\partial \Phi_p}{\partial \mathbf{\nu}}(\mathbf{r}|\mathbf{r}') ds' - \frac{1}{2} f(\mathbf{r}) \quad (H\text{-pol.}). \quad (12b)$$

The integral equation (12b) was obtained using the jump relations of the single layer potential [18]. These jump relations state that the normal derivative of the single-layer potential is discontinuous, i.e., its value calculated from the outer side of ∂D is different from the value calculated from the inner side. In fact, the normal derivative calculated from the exterior of ∂D is equal

to the two right-most parcels in (12b), while the normal derivative calculated from the interior is obtained from the former by replacing the term $-f(\mathbf{r})/2$ by $+f(\mathbf{r})/2$, [18].

We define the integral operators (over ∂D) \mathbf{L} , \mathbf{M}_+ , and \mathbf{M}_- as follows:

$$\mathbf{L}f = \int_{\partial D} f(\mathbf{r}') \Phi_p(\mathbf{r}|\mathbf{r}') d\mathbf{s}' \quad (13a)$$

$$\mathbf{M}_{\pm}f = \int_{\partial D} f(\mathbf{r}') \frac{\partial \Phi_p}{\partial \nu}(\mathbf{r}|\mathbf{r}') d\mathbf{s}' - \left(\pm \frac{1}{2} f(\mathbf{r}) \right) \quad (13b)$$

From (12), we conclude that, provided \mathbf{L} and \mathbf{M}_+ are invertible, we have

$$\begin{aligned} f &= -\mathbf{L}^{-1}\phi \quad (\text{E-polarization}) \\ f &= -\mathbf{M}_+^{-1} \frac{\partial \phi}{\partial \nu} \quad (\text{H-polarization}). \end{aligned} \quad (14a)$$

Finally, from (4) and (11a), we conclude that ϕ is a solution of the following homogeneous equation:

$$\nabla^2\phi + \beta^2 \left(\phi + \int_{\partial D} f \Phi_p d\mathbf{s}' \right) = 0 \quad (14b)$$

$$\phi \exp(j\mathbf{k} \cdot \mathbf{r}) \text{ is periodic.} \quad (14c)$$

Thus, we have proven that to every solution ψ of the extended problem corresponds a solution ϕ of the integral-differential system (14). The mapping that transforms ψ into ϕ is defined by (11). Reciprocally, it is easy to verify that to every solution ϕ of the integral-differential system (14) corresponds a solution ψ of the extended problem. The respective inverse mapping is defined by (11a) and (14). Furthermore, function ψ is a non-trivial solution of the extended problem if and only if the corresponding ϕ is a nontrivial solution of (14). Hence, it follows that both problems are equivalent.

The integral-differential system (14) is also an eigenvalue problem. In fact, for a given wave vector \mathbf{k} , it has nontrivial solutions only for certain wavenumbers β . As pointed out above, the nontrivial solutions of system (14) lead to nontrivial solutions of the extended problem (and reciprocally). Thus, we conclude that both problems have the same band structure. However, the eigenfunctions of (14) are much smoother than the eigenfunctions of the extended problem. In fact, they have continuous derivatives up to order two (inclusive), while, in general, the eigenfunctions of the extended problem have discontinuous first-order derivatives. Due to the referred regularity, the eigenfunctions of (14) can be expanded into a fast converging Fourier series. In this way, the band structure of (14) can be efficiently calculated by means of the plane-wave method.

C. Numerical Solution of (14)

Since ϕ is a smooth Floquet wave, we expand it in a Fourier (pseudoperiodic) series

$$\phi(\mathbf{r}) = \sum_{\mathbf{J}} c_{\mathbf{J}} g_{\mathbf{J}}(\mathbf{r}). \quad (15)$$

In (15), $\mathbf{J} = (j_1, j_2)$ is a multiindex of arbitrary integers, $c_{\mathbf{J}}$ is a constant, and $g_{\mathbf{J}}$ is a plane wave

$$g_{\mathbf{J}}(\mathbf{x}) = \frac{1}{\sqrt{V_{\text{cell}}}} e^{-j\mathbf{k}_{\mathbf{J}} \cdot \mathbf{x}} \quad (16a)$$

$$\mathbf{k}_{\mathbf{J}} = \mathbf{k} + j_1 \mathbf{b}_1 + j_2 \mathbf{b}_2 \quad (16b)$$

where $V_{\text{cell}} = |\mathbf{a}_1 \times \mathbf{a}_2|$ is the area of the unit cell. Replacing (15) in (14b), multiplying the resulting equation by $g_{\mathbf{I}}^*$ (where \mathbf{I}

is an arbitrary multiindex, and the symbol “*” refers to complex conjugation), and integrating both sides over the unit cell Ω , we conclude that

$$-\frac{1}{\beta^2} c_{\mathbf{I}} |\mathbf{k}_{\mathbf{I}}|^2 + c_{\mathbf{I}} + \int_{\partial D} f \langle g_{\mathbf{I}} | \Phi_p \rangle d\mathbf{s}' = 0 \quad (17a)$$

$$\langle g_{\mathbf{I}} | \Phi_p \rangle = \frac{1}{\sqrt{V_{\text{cell}}}} \int_{\Omega} \Phi_p(\mathbf{r}|\mathbf{r}') e^{j\mathbf{k}_{\mathbf{I}} \cdot \mathbf{r}} d^2 \mathbf{r}. \quad (17b)$$

Using (A2), given in the Appendix, we can integrate (17b) explicitly. We find that

$$\langle g_{\mathbf{I}} | \Phi_p \rangle = \frac{1}{|\mathbf{k}_{\mathbf{I}}|^2} g_{\mathbf{I}}^*(\mathbf{r}'). \quad (18)$$

Inserting (18) into (17a), we now obtain

$$\frac{1}{|\mathbf{k}_{\mathbf{I}}|^2} c_{\mathbf{I}} + \frac{1}{|\mathbf{k}_{\mathbf{I}}|^4} \langle g_{\mathbf{I}} | f \rangle_{\partial D} = \frac{1}{\beta^2} c_{\mathbf{I}}. \quad (19)$$

In the previous equation, we defined the internal product $\langle g | h \rangle_{\partial D} = \int_{\partial D} g^* h ds$, where g and h are arbitrary functions defined on the boundary of the inclusion ∂D . Using (14) and (15), we obtain the final result

$$\frac{1}{|\mathbf{k}_{\mathbf{I}}|^2} c_{\mathbf{I}} - \frac{1}{|\mathbf{k}_{\mathbf{I}}|^4} \sum_{\mathbf{J}} c_{\mathbf{J}} \langle g_{\mathbf{I}} | \mathbf{L}^{-1} g_{\mathbf{J}} \rangle_{\partial D} = \frac{1}{\beta^2} c_{\mathbf{I}} \quad (\text{E-pol.}) \quad (20a)$$

$$\frac{1}{|\mathbf{k}_{\mathbf{I}}|^2} c_{\mathbf{I}} - \frac{1}{|\mathbf{k}_{\mathbf{I}}|^4} \sum_{\mathbf{J}} c_{\mathbf{J}} \left\langle g_{\mathbf{I}} \left| \mathbf{M}_+^{-1} \frac{\partial g_{\mathbf{J}}}{\partial \nu} \right. \right\rangle_{\partial D} = \frac{1}{\beta^2} c_{\mathbf{I}} \quad (\text{H-pol.}) \quad (20b)$$

Equation (20) defines an eigensystem with eigenvalues $1/\beta^2$. To solve it numerically, we truncate the Fourier series (15) and discretize the integral operators (13) using, for example, the Nyström method, which is particularly efficient in the analysis of two-dimensional problems [18].

D. Band Structure of the Metallic Crystal

As referred in Section II-A, the band structure of the metallic crystal is obtained from the band structure of the extended problem by removing the flat bands. The band structure of the extended problem is calculated solving the matrix eigensystem (20).

The flat bands are associated to the resonant frequencies of the internal Dirichlet modes. When the inclusion area fraction is low, the internal resonant frequencies are high and, consequently, do not interfere with the first bands of the metallic crystal. The flat bands can be extracted from the band structure of the extended problem using one of the following techniques.

- The simpler one consists of directly detecting the dispersionless flat bands in the computed band structure. Generally, this approach works well, but some ambiguity may arise in metallic crystals with very flat bands.
- A second alternative consists of precalculating the internal mode frequencies, using the fact that the internal modes vanish outside the inclusion (for canonical inclusion cross sections, these frequencies may even be known analytically). This approach is developed in what follows, and is partially related to results from [11].

In a first step, we compute the resonant frequencies of the extended problem with an arbitrary \mathbf{k} - and E -polarization (independently of the metallic crystal polarization case; this is so

because, as we have referred to before, the internal resonant frequencies are common to both polarization cases).

From the eigenvectors of (20a), we obtain the eigenfunctions of (14), which are given by the Fourier expansion (15). Let ϕ be one of these eigenfunctions. Suppose that ϕ has wavenumber β and that we want to test whether or not β corresponds to an internal mode of the extended problem. From (11a) and (14a), the mode of the extended problem associated to ϕ is given by

$$\psi(\mathbf{r}) = \phi(\mathbf{r}) - \int_{\partial D} \mathbf{L}^{-1} \phi \Phi_p(\mathbf{r}|\mathbf{r}') ds'. \quad (21)$$

Thus, the wavenumber β corresponds to an internal mode if and only if ψ given by the previous formula vanishes over $\Omega - D$. From the jump relations of the single-layer potential [18], the normal derivatives of ψ over ∂D are given by

$$\frac{\partial \psi^\pm}{\partial \mathbf{v}} = \frac{\partial \phi}{\partial \mathbf{v}} - \mathbf{M}_\pm \mathbf{L}^{-1} \phi \quad (22)$$

where $\partial \psi^+ / \partial \mathbf{v}$ is the normal derivative of ψ on the outer side of ∂D , and $\partial \psi^- / \partial \mathbf{v}$ is the normal derivative of ψ on the inner side of ∂D .

If the wavenumber β corresponds to an internal mode, it is clear from the above discussion that $\partial \psi^+ / \partial \mathbf{v} = 0$ and $\partial \psi^- / \partial \mathbf{v} \neq 0$. Similarly, as every noninternal solution of the E -polarization extended problem vanishes in the interior of the metallic inclusions, the noninternal modes satisfy $\partial \psi^+ / \partial \mathbf{v} \neq 0$ and $\partial \psi^- / \partial \mathbf{v} = 0$.

From the preceding considerations, we propose the following criterion to decide whether the resonant wavenumber β does or does not correspond to an internal mode. A resonant wavenumber β is labeled as internal if the norm [with respect to the internal product on ∂D defined in (19)] of $\partial \psi^+ / \partial \mathbf{v}$ is much smaller than the norm of $\partial \psi^- / \partial \mathbf{v}$. If the norm of $\partial \psi^+ / \partial \mathbf{v}$ is much greater than $\partial \psi^- / \partial \mathbf{v}$, the mode is labeled as noninternal. If the norms of the normal derivatives have approximately the same magnitude, there is some ambiguity. The ambiguity is, in general, due to a lack of numerical resolution (although some degeneracy may occur if some noninternal mode has a resonant frequency very close to that of an internal mode). To remove the ambiguity, if it occurs at all, it is, in general, sufficient to increase the number of plane waves in expansion (14). We note, however, that we only need to accurately determine the first few internal resonant frequencies, more precisely, those that lie in the frequency range where we wish to determine the band structure of the metallic crystal. Every resonant wavenumber labeled as internal (if any) is stored in memory.

In a second step, we calculate the band structure of the metallic crystal by performing the usual \mathbf{k} sweeping of the Brillouin zone. Toward this end, the eigensystem (20) is solved for several wave vectors \mathbf{k} . The internal resonant frequencies (which were previously stored in memory) are removed from the band structure yielded by (20). It must be pointed out that, due to the involved numerical approximations, the stored internal frequencies are not exactly reproduced in the calculated band structure. In fact, the removed eigenvalues are those that are closer to the stored internal frequencies.

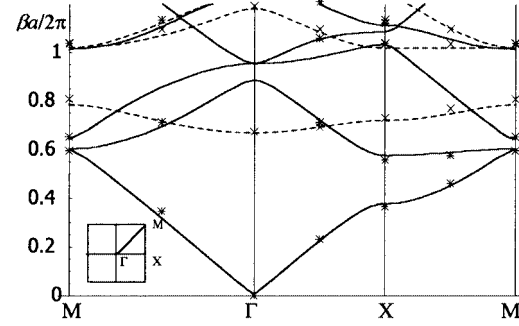


Fig. 2. Band structure for a square array of circular cylinders with fill fraction 21.2%. E -polarization (dashed line) and H -polarization (solid line) superimposed on the results from [13].

III. NUMERICAL RESULTS

In this section, we present numerical examples that illustrate the application of the described method.

The results presented here were calculated using 49 terms in the plane-wave expansion (15). The integral operators, defined by (13), were discretized using the Nyström method with 32 points on the inclusion's boundary. For each \mathbf{k} in the Brillouin zone, the computation time is less than 1 s on a Pentium III 800 MHz.

In the first example, we calculate the band structure of a square array of PEC circular cylinders in air. The lattice constant is a and the cylinder area fraction is 21.2%. In Fig. 2, we present the first few bands of each polarization, superimposed on data extracted from [13] (the crosses correspond to the E -polarization points extracted from [13], while the stars correspond to the H -polarization points). The inset of Fig. 2 represents the Brillouin zone of the square lattice. Point Γ is the origin of the \mathbf{k} -space, and points M and X are given, respectively, by $X = 0.5\mathbf{b}_1$ and $M = 0.5(\mathbf{b}_1 + \mathbf{b}_2)$. The computation time of the data extracted from [13] is 16 h on a DEC Alpha Workstation. As illustrated in Fig. 2, the calculated results agree well with those of [13].

In the E -polarization case, the cutoff free-space wavelength is $\lambda_c = 2\pi/\beta = a/0.67$, i.e., $\lambda_c = 1.49a$. Thus, for this polarization, only wavelengths smaller than $1.49a$ can propagate in the metallic crystal. In the long wavelength limit, the medium can be modeled as plasma with negative permittivity.

On the other hand, in the H -polarization case and long wavelengths, the medium behaves as a natural medium characterized by a permittivity dyadic and magnetic permeability. Thus, the artificial medium can be used as a polarizer that inhibits E -polarization and is transparent to H -polarization.

In order to investigate the accuracy and convergence rate of the proposed method, we have calculated the relative error in the frequency of the first internal mode, as a function of $\sqrt{N_p}$, where N_p is the number of plane waves in expansion (15). Since, in the present example, the inclusion's cross section is circular, the referred frequency is known in closed analytical form [17]. For the fill fraction 21.2%, the corresponding normalized wavenumber satisfies $\beta a = 9.26$. We have compared this value with that obtained from the numerical results. We discretized the integral operators with 32 points on ∂D and

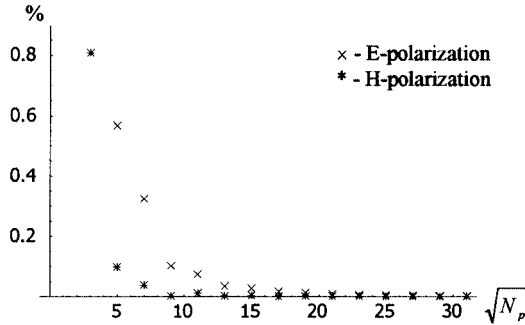


Fig. 3. Relative error (in percentage) in the resonant frequency of the first internal mode as a function of the square root of the number of plane waves.

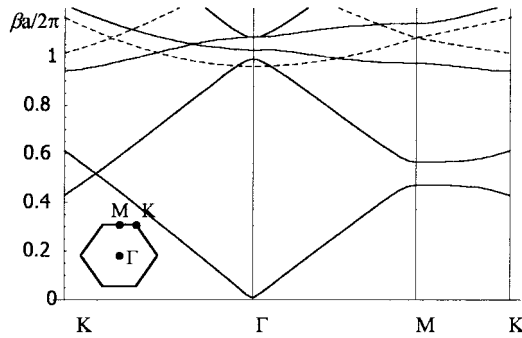


Fig. 4. Band structure for a triangular array of elliptical cylinders with a fill fraction of 35%. *E*-polarization (dashed line). *H*-polarization (solid line).

considered that $\mathbf{k} = 0.05\mathbf{b}_1$. In the *E*-polarization case, the first internal frequency is the sixth resonant frequency of the extended problem, while in the *H*-polarization case, it is the ninth resonant frequency. The calculated relative error is shown in Fig. 3. The accuracy of the computed results is excellent. The relative error is less than 0.6% for $\sqrt{N_p} \geq 5$. The convergence rate is also very good, irrespective of the polarization case.

In the second example (Fig. 4), we consider a triangular lattice, with lattice constant a (i.e., the primitive vectors \mathbf{a}_1 and \mathbf{a}_2 make an angle of 60° and have a norm a ; we assume that \mathbf{a}_1 is oriented in the x_1 -axis direction). The inclusions are now metallic cylinders with an elliptical cross section. The area fill fraction is 35%, and the axis ratio of the elliptical cross section is two. The Brillouin zone of the triangular lattice is the hexagon shown in the inset of Fig. 4. Also shown are the points Γ (the origin of the \mathbf{k} -space), $M = 0.5\mathbf{b}_2$, and K is the upper right corner of the regular hexagon. The larger axis of the elliptical cross section is oriented in the ΓK -direction.

The free-space cutoff wavelength for the *E*-polarization case increases relatively to the previous example, and is now $\lambda_c = a/0.96 = 1.04a$. There is no bandgap in the *H*-polarization case and, for long wavelengths, the medium behaves as an anisotropic effective medium. We verified that, except near the ΓK -direction, there is a bandgap between the first and second bands of the *H*-polarization. The reason for the bandgap absence in the ΓK -direction seems to be that the elliptical cylinders form to a first approximation a guided-wave structure (of parallel metallic plates) oriented in the ΓK -direction. This is so because the ellipse larger axis is oriented in the ΓK -direction.

IV. CONCLUSIONS

We have presented a new method for the efficient calculation of the band structure of arrays of PEC cylinders with arbitrary cross section. We derived an auxiliary integral-differential eigensystem that contains the band structure of the metallic crystal. It was shown that, due to the smoothness of eigenfunctions of the auxiliary problem, its band structure could be computed very efficiently using the plane-wave method. In this way, we have reduced the problem of calculating the band structure of PEC metallic crystals to a conventional matrix eigensystem. This approach is far more efficient than other root-searching methods presented in the literature. Typical computation times, even for highly concentrated systems, and a high-accuracy specification for the first few bands, are less than 1 s in a standard personal computer. In fact, due to the smoothness of the eigenfunctions, the plane-wave expansion method converges fast, and only a few plane waves are needed to yield accurate results. The theoretical results were validated with numerical results available from the open literature.

The extension of the proposed method to the three-dimensional problem, and dielectric crystals, will appear shortly.

APPENDIX

In this section, we present closed-form formulas for the solution of (7). That solution corresponds to the $\beta = 0$ case of the more general equation

$$\nabla^2 \Phi_p + \beta^2 \Phi_p = -e^{-j\mathbf{k} \cdot (\mathbf{r} - \mathbf{r}')} \sum_{\mathbf{I}} \delta(\mathbf{r} - \mathbf{r}' - \mathbf{r}_{\mathbf{I}}) \quad (\text{A1a})$$

$$\Phi_p \exp(j\mathbf{k} \cdot (\mathbf{r} - \mathbf{r}')) \text{ is a periodic} \quad (\text{A1b})$$

where β is a given wavenumber. We refer to Φ_p as the “lattice Green function.” A well-known representation of this pseudoperiodic Green function is given in [19]

$$\Phi_p(\mathbf{u}) = \frac{1}{V_{\text{cell}}} \sum_{\mathbf{J}} \frac{e^{-j\mathbf{k}_{\mathbf{J}} \cdot \mathbf{u}}}{|\mathbf{k}_{\mathbf{J}}|^2 - \beta^2} \quad (\text{A2a})$$

$$\mathbf{k}_{\mathbf{J}} = \mathbf{k} + j_1 \mathbf{b}_1 + j_2 \mathbf{b}_2 \quad (\text{A2b})$$

where $\mathbf{J} = (j_1, j_2)$ is a multiindex of integers, V_{cell} is the area of the unit cell, and $\mathbf{u} = (u_1, u_2) = \mathbf{r} - \mathbf{r}'$. The convergence rate of (A2) is poor. Next, we derive an alternative representation for Φ_p with exponential convergence. The final result is

$$\Phi_p(\mathbf{u}) = \frac{1}{|\mathbf{a}_1|} \sum_n \frac{e^{-j\mathbf{K}_{n, //} \cdot \mathbf{u}}}{2\gamma_n} \cdot \left(e^{-\gamma_n |u_{\perp}|} + \sum_{\pm} \frac{e^{\pm\gamma_n u_{\perp}}}{e^{|a_{2\perp}|(\gamma_n \pm jK_{n, \perp})} - 1} \right) \quad (\text{A3a})$$

$$\gamma_n = \sqrt{|\mathbf{K}_{n, //}|^2 - \beta^2} \quad (\text{A3b})$$

where $\mathbf{K}_n = \mathbf{k} + n\mathbf{b}_1$, $\mathbf{K}_{n, //}$ is the projection of \mathbf{K}_n onto the \mathbf{a}_1 -direction, and $K_{n, \perp}$, $a_{2\perp}$, and u_{\perp} are, respectively, the projections of \mathbf{K}_n , \mathbf{a}_2 , and \mathbf{u} onto a unit vector normal to \mathbf{a}_1 . In (A3a), the sum with index “ \pm ” is the shorthand notation for the sum of two terms: one with the “+” sign and the other with the “-” sign.

Formula (A3) is only valid for $|u_{\perp}| < |a_{2\perp}|$. However, since Φ_p is a pseudoperiodic function, we can relate Φ_p calculated in an arbitrary point \mathbf{u} , with Φ_p calculated in a point $\tilde{\mathbf{u}}$ obtained from \mathbf{u} by translations along the primitive vectors. As we can always choose $\tilde{\mathbf{u}}$ such that it satisfies $|\tilde{u}_{\perp}| < |a_{2\perp}|/2$, Φ_p can be evaluated in an arbitrary point of space.

The demonstration of (A3) is as follows. The Green function Φ_p is the potential from a two-dimensional array of point sources, with phase shifts imposed by \mathbf{k} . The two-dimensional array can be regarded as the superimposition of one-dimensional arrays point sources. The potential from each one-dimensional array is a “layer Green function.” This “layer Green function” is the usual periodic Green function used in the analysis of single-periodic structures in a two-dimensional space [20]. The Green function Φ_p can thus be written as a sum of “layer Green functions.” Using the spectral representation of the “layer Green function” [20], we can verify that the sum of the layer potentials corresponds to two geometric series and, thus, can be evaluated in closed form. The result is (A3).

The representation (A3) converges exponentially, except when $u_{\perp} = 0$. Nevertheless, it is obvious that, by interchanging the roles of \mathbf{a}_1 and \mathbf{a}_2 in (A3), we obtain an alternative representation for Φ_p . This second representation is analogous to the first one, but the region of slow convergence differs. In fact, it can be verified that for every \mathbf{u} in the unit cell, at least one of these representations converges exponentially, except if $\mathbf{u} = \mathbf{0}$. At the origin, Φ_p diverges, and has the same logarithmic singularity as the free-space Green function. Near $\mathbf{u} = \mathbf{0}$, we can write $\Phi_p = \Phi_0 + \Phi_{\text{reg}}$, where Φ_0 is the free-space Green function and Φ_{reg} is a regular term. Alternatively, we can accelerate the convergence of (A3) using the usual techniques employed for the “layer Green function” [20]. In fact, the first term of (A3a) (the one that converges slowly) is precisely the “layer Green function.”

REFERENCES

- [1] E. Yablonovitch, T. J. Gmitter, and K. M. Leung, “Photonic band structure: The FCC case employing nonspherical atoms,” *Phys. Rev. Lett.*, vol. 67, p. 2295, Oct. 1991.
- [2] M. Silveirinha and C. A. Fernandes, “Design of printed disk artificial materials,” in *Proc. IEEE AP-S/URSI Symp.*, vol. 4, San Antonio, TX, June 2002, pp. 352–355.
- [3] ———, “Effective permittivity of metallic crystals: A periodic Green’s function formulation,” *Electromagnetics (Special Issue)*, 2003, to be published.
- [4] C. T. Chan, Q. L. Yu, and K. M. Ho, “Order- N spectral method for electromagnetic waves,” *Phys. Rev. B, Condens Matter*, vol. 51, p. 16635, 1995.
- [5] J. B. Pendry and A. MacKinnon, “Calculation of photon dispersion relations,” *Phys. Rev. Lett.*, vol. 69, p. 2772, 1992.
- [6] H. Y. Yang, “Finite difference analysis of 2-D photonic crystals,” *IEEE Trans. Microwave Theory Tech.*, vol. 44, p. 2688, Dec. 1996.
- [7] K. M. Ho, C. T. Chan, and C. M. Soukoulis, “Existence of a photonic gap in periodic dielectric structures,” *Phys. Rev. Lett.*, vol. 65, p. 3152, Dec. 1990.
- [8] H. S. Sozuer, J. W. Haus, and R. Inguva, “Photonic bands: Convergence problems with the plane-wave method,” *Phys. Rev. B, Condens. Matter*, vol. 45, pp. 13 962–13 972, June 1992.
- [9] P. R. Villeneuve and M. Piché, “Photonic bandgaps: What is the best numerical representation of periodic structures?,” *J. Mod. Opt.*, vol. 41, pp. 241–256, 1994.
- [10] M. Silveirinha and C. A. Fernandes, “An hybrid method for the calculation of the band structure of 2D photonic crystals,” in *Proc. IEEE AP-S/URSI Symp.*, vol. 4, San Antonio, TX, June 2002, pp. 348–351.
- [11] G. Conciauro, P. Arcioni, M. Bressan, and L. Perregiani, “Wideband modeling of arbitrarily shaped H -plane waveguide components by the ‘boundary integral-resonant mode expansion method’,” *IEEE Trans. Microwave Theory Tech.*, vol. 44, pp. 1057–1066, July 1996.
- [12] P. Arcioni, M. Bressan, G. Conciauro, and L. Perregiani, “Wideband modeling of arbitrarily shaped E -plane waveguide components by the boundary integral-resonant mode expansion method,” *IEEE Trans. Microwave Theory Tech.*, vol. 44, pp. 2083–2092, Nov. 1996.
- [13] N. A. Nicorovici, R. C. McPhedran, and L. C. Botten, “Photonic band gaps for arrays of perfectly conducting cylinders,” *Phys. Rev. E, Stat. Phys. Plasmas Fluids Relat. Interdiscip. Top.*, vol. 52, pp. 1135–1145, 1995.
- [14] D. R. Smith, S. Schultz, N. Kroll, M. Sigalas, K. M. Ho, and C. M. Soukoulis, “Experimental and theoretical results for a two-dimensional metal photonic band-gap cavity,” *Appl. Phys. Lett.*, vol. 65, pp. 645–647, 1994.
- [15] M. M. Sigalas, C. T. Chan, K. M. Ho, and C. M. Soukoulis, “Metallic photonic band-gap materials,” *Phys. Rev. B, Condens. Matter*, vol. 52, pp. 11 744–11 751, 1995.
- [16] K. Sakoda, *Optical Properties of Photonic Crystals*, ser. Opt. Sci. 80. Berlin, Germany: Springer-Verlag, 2001.
- [17] R. E. Collin, *Field Theory of Guided Waves*, 2nd ed. New York: IEEE Press, 1991.
- [18] D. Colton and R. Kress, *Inverse Acoustic and Electromagnetic Scattering Theory*. Berlin, Germany: Springer-Verlag, 1992.
- [19] N. A. Nicorovici, R. C. McPhedran, and B. Ke-Da, “Propagation of electromagnetic waves in periodic lattices of spheres: Green’s function and lattice sums,” *Phys. Rev. E, Stat. Phys. Plasmas Fluids Relat. Interdiscip. Top.*, vol. 51, pp. 690–702, 1995.
- [20] R. Jorgenson and R. Mittra, “Efficient calculation of the free-space periodic Green’s function,” *IEEE Trans. Antennas Propagat.*, vol. 38, pp. 633–642, May 1990.

Mário G. Silveirinha (S’99) was born in Portugal, in 1975. He received the Licenciado degree in electrical engineering from the University of Coimbra, Coimbra, Portugal, in 1998, and is currently working toward the Ph.D. degree in electrical engineering at the Technical University of Lisbon, Lisbon, Portugal.

His research interests include propagation in periodic structures and lens antennas.

Carlos A. Fernandes (S’86–M’89) received the Licenciado, M.Sc., and Ph.D. degrees in electrical and computer engineering from the Instituto Superior Técnico (IST), Technical University of Lisbon, Lisbon, Portugal, in 1980, 1985, and 1990, respectively.

In 1980, he joined the IST, where, since 1993, he has been an Associate Professor with the Department of Electrical and Computer Engineering in the areas of microwaves, radio-wave propagation, and antennas. Since 1993, he has also been a Senior Researcher with the Instituto de Telecomunicações, where he is currently the Coordinator of the wireless communications scientific area. He has been the leader of antenna activity in national and European projects such as RACE 2067–MBS (Mobile Broadband System), and ACTS AC230–SAMBA (System for Advanced Mobile Broadband Applications). He has coauthored a book, a book chapter, and several technical papers in international journals and conference proceedings in the areas of antennas and radio-wave propagation modeling. His current research interests include artificial dielectrics, dielectric antennas for millimeter-wave applications, and propagation modeling for mobile communication systems.